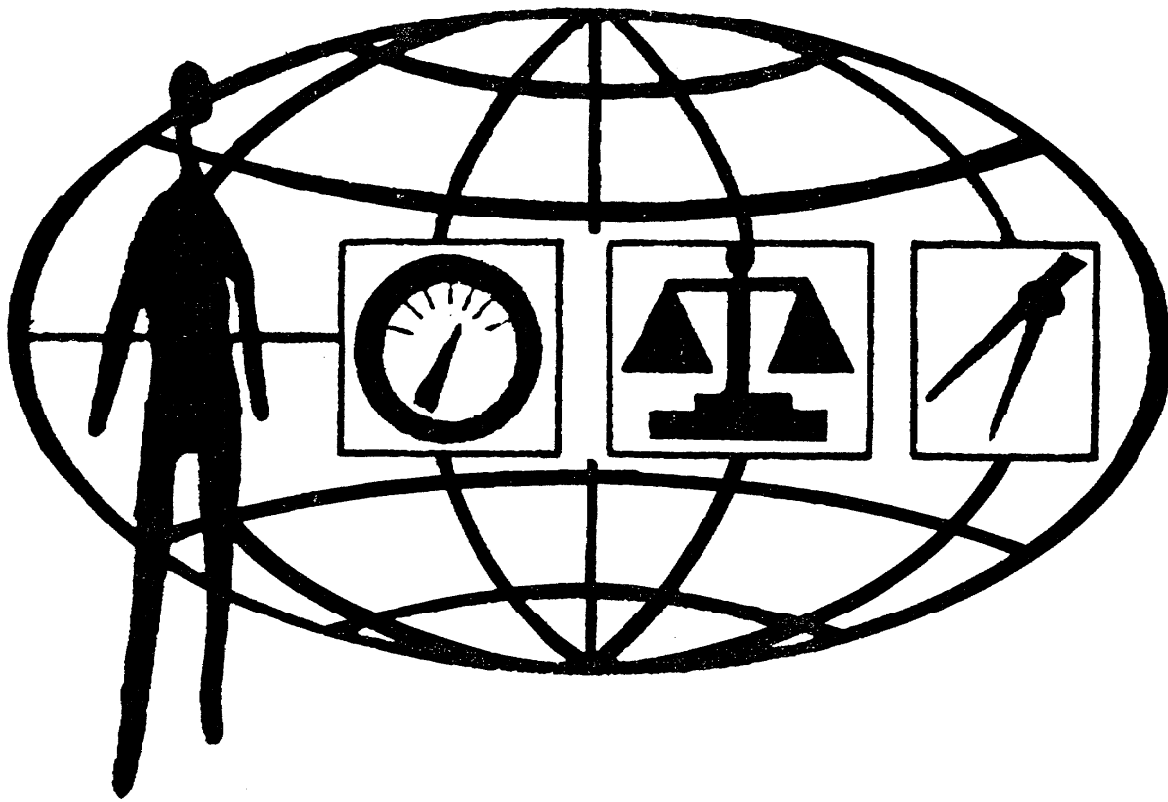

NATIONAL
CONFERENCE OF
STANDARDS
LABORATORIES



1983 Workshop
and Symposium

The Hilton Harvest House
Boulder, Colorado
july 18-21, 1983

AN AUTOMATED SYSTEM FOR THE ABSOLUTE
MEASUREMENT OF PICKUP SENSITIVITY

B. F. Payne and M. R. Serbyn
National Bureau of Standards

A Michelson Interferometer has been adapted to measure the magnitude and phase of the sensitivity characterizing a vibration pickup. The system, controlled by a low-cost desktop computer, is fully automated. It was designed to operate in the frequency range 1-20 kHz, which is determined primarily by the nature of the vibration exciter. The magnitude component of the pickup sensitivity normally is measured at 121.10 nm peak displacement, but higher levels are possible. For the measurement of the phase component, the vibrational displacement should be less than about 120 nm. The chief advantages of the system are its simplicity and economy of instrumentation. This paper describes the operation of the system, shows typical calibration results, and discusses the accuracy and precision of the measurements.

INTRODUCTION

The interferometric method of measuring the amplitude of vibratory motion was already old seventy years ago. In a 1915 paper read before the National Academy of Sciences of the U.S.A., Webster, commenting on absolute acoustical measurements, remarked: "For years all measurements were made by the Michelson interferometer viewed stroboscopically[1]¹." Subsequent investigators visually observed the disappearance of the fringe pattern[2-6], an effect that corresponds to a constant value of the time-averaged intensity. Because of its inherent simplicity and precision, the technique has acquired classical status. In the electronic age, attempts were made to improve the precision of the fringe-disappearance method by eliminating the need for direct visual observation[7]. About ten years ago, one of us used the d-c component as a supplement to the harmonic information contained in the photodetector output[8], but a calibration system based exclusively on the time average of the resultant intensity of the interfering beams has, to our best knowledge, never been implemented, although the feasibility of such a system was demonstrated in two recent communications[9,10].

The present paper describes the automation and qualification of an actual calibration system designed to measure both the magnitude and the phase of a vibration pickup. Figure 1 shows the components of the system. It consists of a Michelson interferometer in which one of the light beams is modulated by the vibration to be measured, while the path length of the other is slowly varied in a cyclic manner by moving the "fixed" mirror. The pickup being calibrated is mounted on top of the vibration exciter. The calibration procedure, controlled by a small desktop computer, will be described in a subsequent section.

THEORY

General

The sensitivity S of a pickup is defined as the ratio of its electrical output E to a mechanical input Q .

$$S = E/Q = E/(2\pi f)^2 d \quad (1)$$

¹ Numbers in [] indicate literature references at the end of this paper.

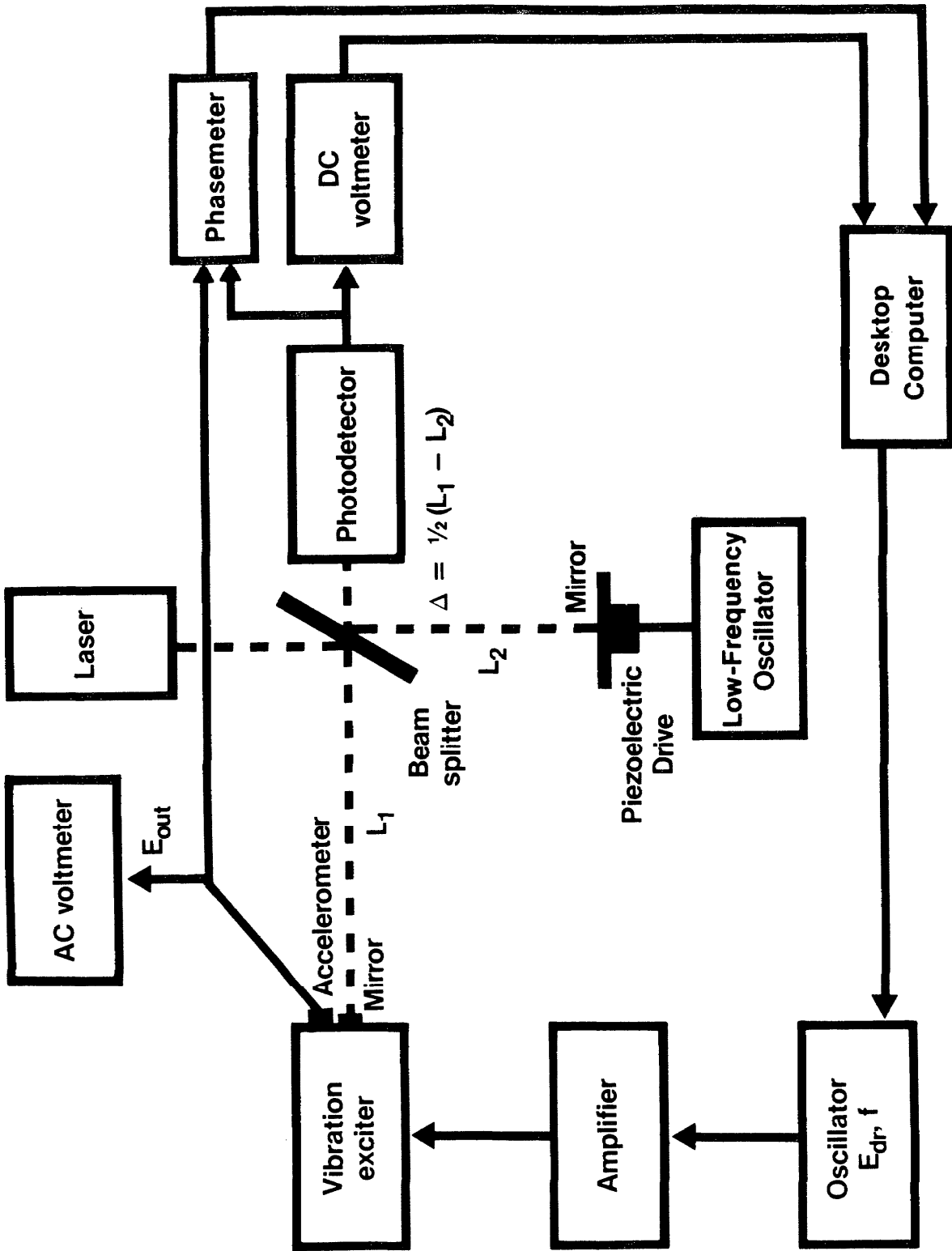


FIGURE 1. Functional diagram of the calibration system

In the case of an accelerometer excited by sinusoidal vibration, $Q = (2\pi f)^2 d$, where f is the frequency and d is the peak value of the vibratory displacement, which for the present method is 121.10 nm. Note that in Eq. (1), both E and Q are phasor quantities; therefore, complete specification of S requires both magnitude and phase. In the United States, it is customary to express acceleration as a multiple of the standard acceleration of free fall, $g = 9.80665 \text{ m/s}^2$. The working formula for sensitivity then becomes

$$S = E / (0.34472f^2) \text{ mV/"g"} , \quad (2)$$

where E is the rms value of the accelerometer output in mV, and f is the vibration frequency in kHz.

Because the value of d in Equation (1) is determined by the wavelength of the light used, the method to be described is classified as absolute. But, strictly speaking, this designation applies only to the displacement measurement, for "absolute" denotes a measurement directly in terms of quantities whose units form the base units of the system [11].

The heart of the measurement system is a two-beam Michelson interferometer, shown in Figure 1. If the difference of its optical path lengths is modulated by periodically vibrating one of its mirrors, both the amplitude and the phase of this modulation are encoded in the intensity of the light impinging on the photodetector. The "fixed" mirror is mounted on a small piezoelectric transducer for the purpose of slowly varying the value of $\Delta = 2(L_1 - L_2)$. These quasi-static changes can be followed by both the d-c voltmeter and the phasemeter.

Let the surface of the vibration exciter move according to the following relation

$$\xi = d \cos(\omega t + \phi) , \quad (3)$$

where ξ is the instantaneous displacement, d is the peak value of the displacement, ω is the angular frequency of the motion, t is time, and ϕ is the phase of the displacement relative to some convenient reference, which in the present application is the voltage signal of the pickup being calibrated.

The instantaneous current flowing in the output resistor of the photodetector is

$$i = A + B \cos(4\pi\Delta/\lambda) \left\{ J_0(4\pi d/\lambda) - 2J_2(4\pi d/\lambda) \cos 2(\omega t + \phi) + \dots \right\} \\ - B \sin(4\pi\Delta/\lambda) \left\{ 2J_1(4\pi d/\lambda) \cos(\omega t + \phi) - 2J_3(4\pi d/\lambda) \cos 3(\omega t + \phi) + \dots \right\} , \quad (4)$$

where A and B are constants of the interferometer, λ is the wavelength of the light source (632.82 nm for the He-Ne laser used by the authors), and $J_p(x)$ are Bessel functions of the first kind of order p. Equation (4), with slight changes of notation², corresponds to Equation (1) of Reference 12.

The time average of the light intensity accounts for the first two terms of Equation (4); thus

$$I_{dc} = A + B \cos(4\pi\Delta/\lambda) J_0(4\pi d/\lambda) . \quad (5)$$

This component contains the magnitude of the displacement d, but yields no phase information. The latter appears in each of the harmonic terms. In particular, consider the fundamental component of the photodetector output

$$i_1 = -2B \sin(4\pi\Delta/\lambda) J_1(4\pi d/\lambda) \cos(\omega t + \phi) . \quad (6)$$

Whenever the coefficient of $\cos(\omega t + \phi)$ is positive, the phase of i_1 is the same as the phase of ξ .

Magnitude of S

Equation (5) provides the basis for this measurement, and Figure 1 shows the instrumentation. A low-frequency (0.1-0.2 Hz) sinusoidal or triangular sweep is applied to the piezoelectric mirror-drive, which causes periodic changes in Δ . These changes produce a slowly varying component in the photodetector output. As pointed out earlier, this component contains the displacement amplitude d, within the argument of the Bessel function $J_0(4\pi d/\lambda)$. To extract this information, a d-c voltmeter samples I_{dc} , and the computer calculates

$$M = \max(I_{dc}) - \min(I_{dc}) = 2BJ_0\left(\frac{4\pi d}{\lambda}\right) = 2BJ_0\left(\frac{4\pi \sqrt{2}E}{\lambda \omega^2 |S|}\right) \quad (7)$$

as a function of E.

Since we are ultimately interested in the root of $J_0(4\pi d/\lambda)$, the Bessel function is replaced by the first two terms of its Taylor expansion about the root; hence,

$$M \cong 2B \left\{ (-0.51915) \frac{4\pi \sqrt{2}E}{\lambda \omega^2 |S|} + 1.2484 \right\} . \quad (8)$$

² The sign error at the beginning of line 3 of Equation (1) in Reference 12 has been corrected in the present version.

This equation is of the form $y=mx+b$, with y corresponding to M , and x corresponding to E . The E -intercept, therefore, becomes

$$E|_{M=0} = 2.40482 \frac{\omega^2 \lambda |S|}{4\pi\sqrt{2}} \quad (9)$$

or $|S| = \frac{2.9008}{f^2} E|_{M=0} \text{ mV/"g"}$, (10)

where E and M are measured in mV , and f , in kHz . Equation (10) is the same as Eq. (2), which proves the correctness of the approach. Figure 2 flow charts the measurement procedure. Variation of E is accomplished by programming the oscillator that generates the drive voltage for the vibration exciter. For best results, it is important to make the range of this variation coincide with the most accurate range of Eq. (8). This requires a determination of the sign of M as well as of its magnitude, which is easily achieved by taking advantage of the "V"-like nature of the $|M|$ vs. E curve. As E is increased, $|M|$ decreases until some minimum value, after which it again increases. To correspond with the behavior of $J_0(x)$, the first branch of M is declared positive, the second, negative. The minimum value is discarded.

When an acceptable measurement of the magnitude of S has been made, the computer initiates the measurement of the phase of S . The acceptance criterion is the degree of uncertainty in the E intercept. Table I illustrates the above procedure.

Table I- Sample Data for Calculating $|S|$.

K	$E_{dr}(K)$	$M(K)$	$E(K)$
1	1.335	9.8	121.102
2	1.34	6.2	121.4935
3	1.345	5.2	121.9175
4	1.35	2.8	122.308
(5	1.355	+1.6	122.7465)
6	1.36	-3.1	123.1375
7	1.365	-4.3	123.5695
8	1.37	-6.2	123.959
9	1.375	-6.6	124.397
10	1.38	-8.3	124.791
11	1.385	-11.0	125.2365

Frequency = 6.000 kHz
 E-intercept = 122.8777 mV
 Std. deviation = 0.0699 mV
 Sensitivity = 9.90 mV/"g"

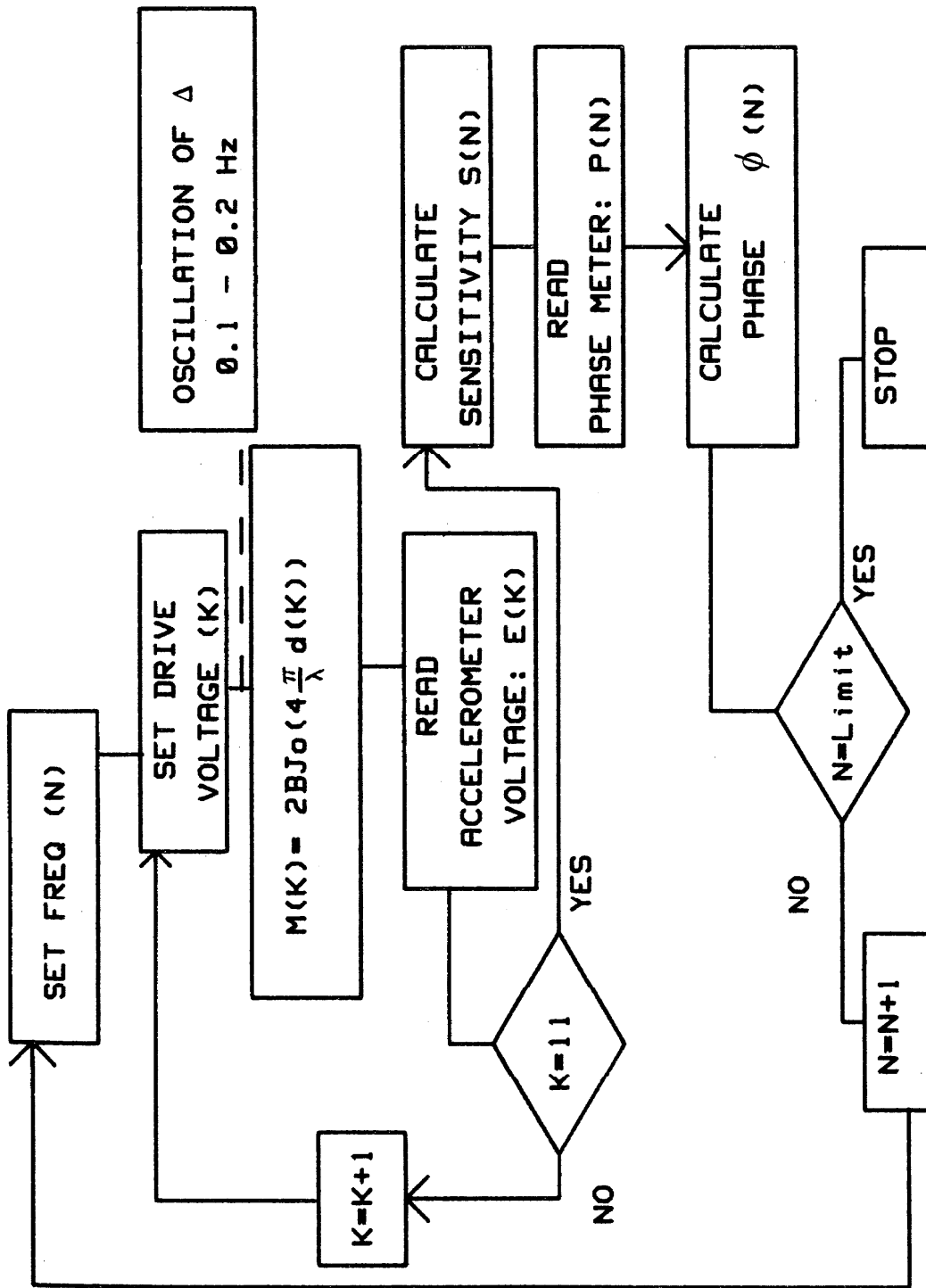


FIGURE 2. Flow chart for the calibration algorithm

Phase of S

It has already been pointed out by Equation (6) that the phase of the vibratory displacement ξ is the same as that of the fundamental component of the photodetector output, provided $-2B\sin(4\pi\Delta/\lambda)J_1(4\pi d/\lambda) > 0$. Since $B > 0$ and $J_1(4\pi d/\lambda) > 0$ for $d < 192.96$ nm, this condition reduces to

$$\begin{aligned} \sin(4\pi\Delta/\lambda) &< 0 \\ \text{or } (2n+1)\lambda/4 &< \Delta < (n+1)\lambda/2, \quad n=0, \pm 1, \pm 2, \dots \end{aligned} \quad (11)$$

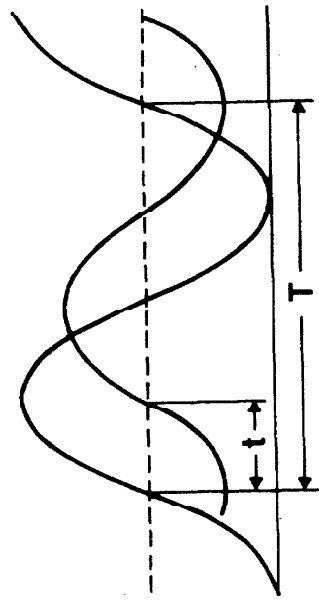
Note that the mid-point of this range,

$$\Delta = (4n+3)\lambda/8, \quad n=0, \pm 1, \pm 2, \dots \quad (12)$$

corresponds to $\sin(4\pi\Delta/\lambda) = -1$. Hence, by adjusting Δ to be near this value, the condition expressed by Eq. (11) can be readily met. When Δ reaches the value prescribed by Eq. (12), the cosine term of the "d-c" component of the photodetector output, given by Eq. (5), goes through zero with a positive slope. This fact provides a simple diagnostic test for the condition expressed by Eq. (12).

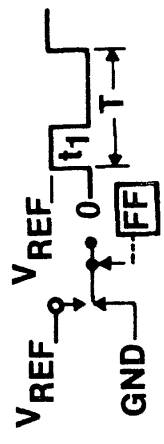
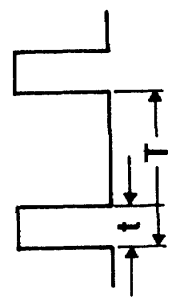
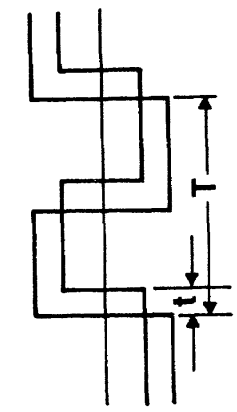
Closer examination of Eq. (4) reveals that, if the range of "d" is suitably restricted, the unfiltered output of the photodetector can be used in place of the fundamental component. Prerequisite to any explanation of this happenstance is an understanding of the principle of phase measurement used in modern phase instruments. This is summarized in Figure 3, which graphically shows how phase is measured by observing the time interval between corresponding zero-crossings of the two waveforms. It should also be clear that waveform details do not affect the result. Thus, the phase differences in (a) and (b) of Figure 4 are the same.

When the phase of i is measured under the condition of Eq. (12), only the odd harmonics are present, which allows d to be as high as about 150 nm and as low as the prevailing noise conditions allow. The high d -limit comes from the behavior of Bessel functions, as shown in Figure 5. It should be pointed out that if the unfiltered photodetector output is used, the true value of phase is measured only when Eq. (12) holds. This is more restrictive than the filtered case, where Δ is limited by the inequality (11). In practice, however, one may still measure the phase during a range of Δ values and expect the true value to be given by the average. To be sure, when the value of Δ departs from that given by Eq. (12), the phase is changed by the appearance of even harmonics (see Figure 6). But these changes cancel themselves out, if care is taken to obtain an equal number of samples on either side of $\Delta = (4n+3)\lambda/8$. This is illustrated by



If t is the time interval between analogous zero-crossings, and T is the wave period, then the phase angle, ϕ , is given by:

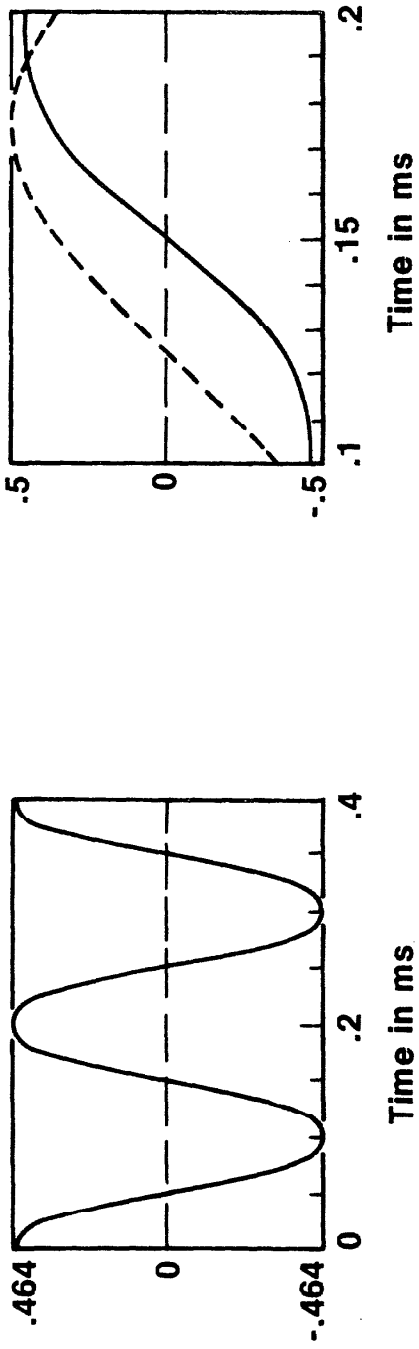
$$\phi = 360 \left(\frac{t}{T} \right) \text{degrees}$$



$$\text{DC average} = \left(\frac{t}{T} \right) V_{\text{REF}}$$

FIGURE 3. Principle of phase measurement used in modern phase instrumentation

(a) $d = 60 \text{ nm}$



(b) $d = 120 \text{ nm}$

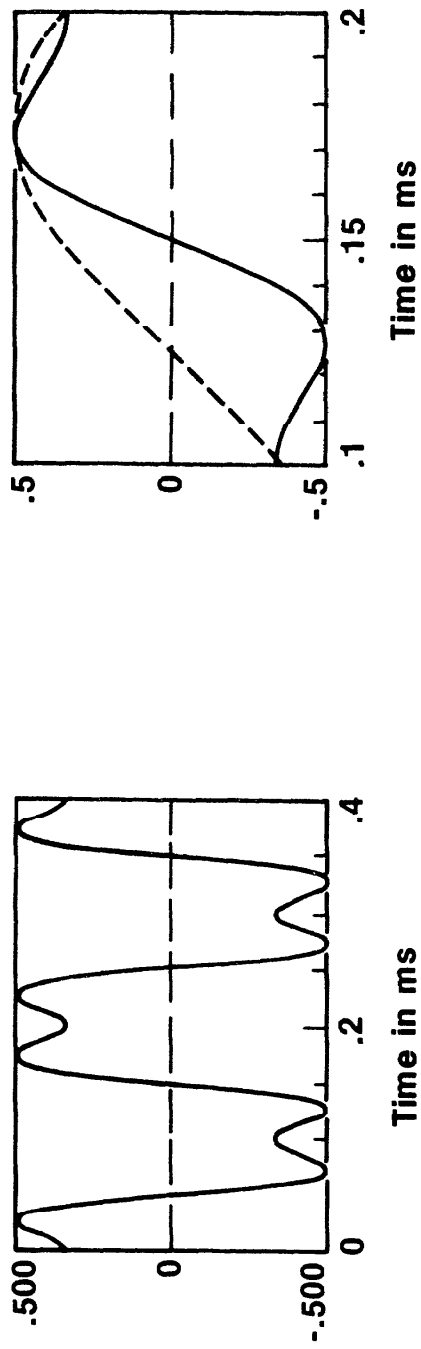


FIGURE 4. Photodetector (solid) and accelerometer

(dashed) outputs at $\Delta = 3 \lambda / 8$

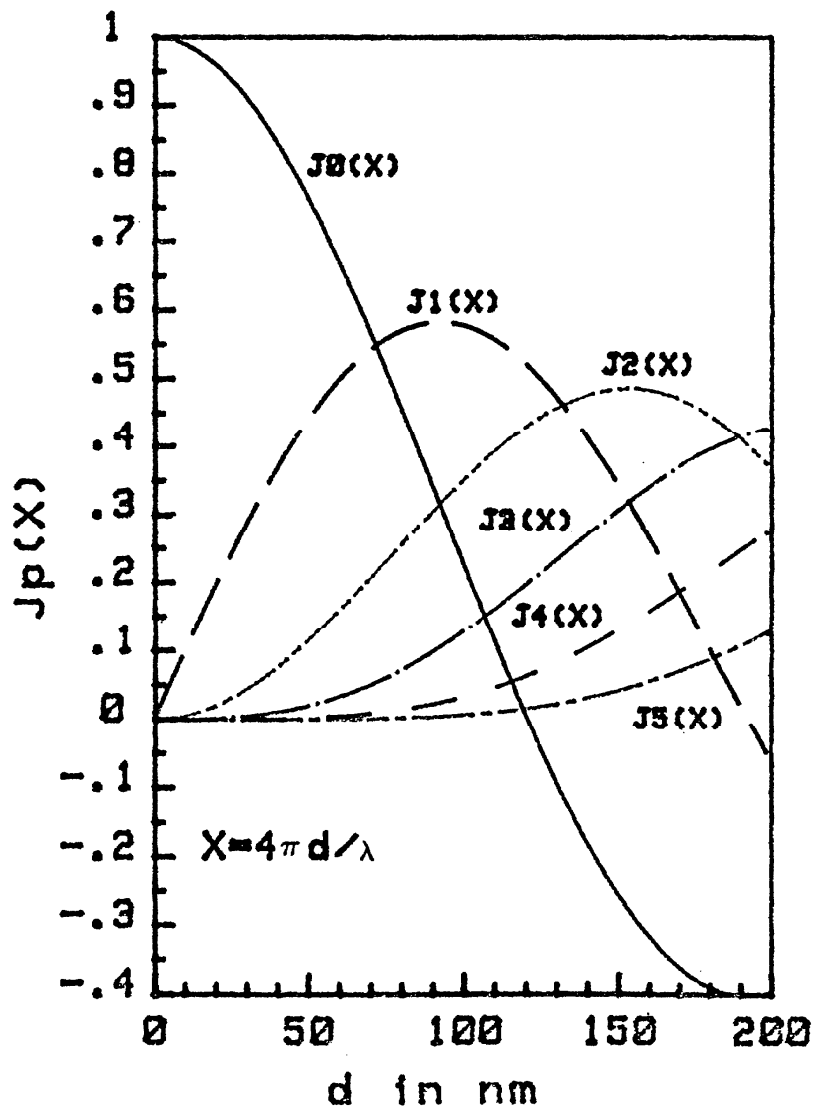
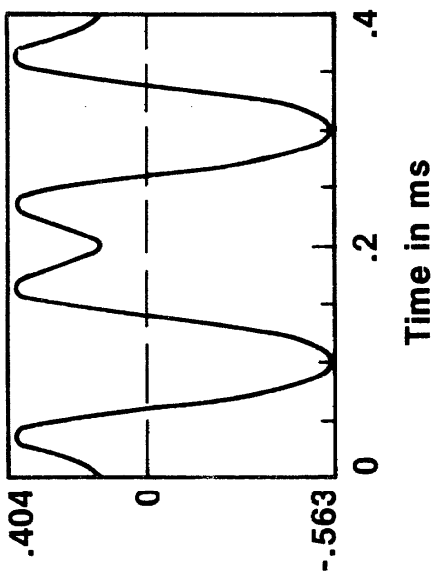
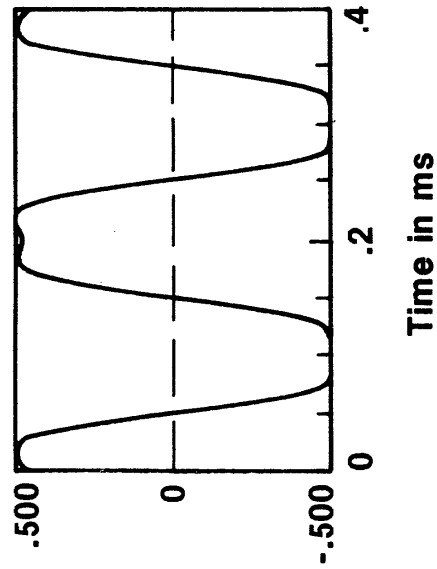
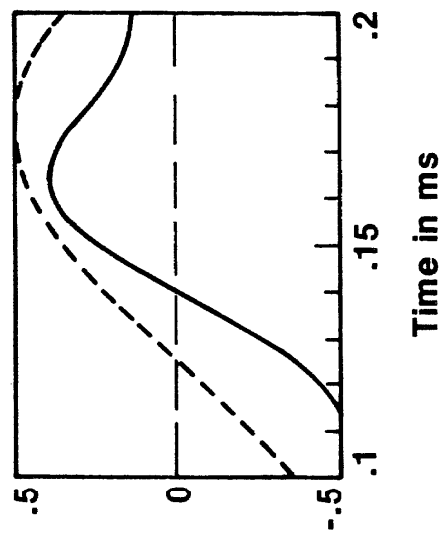


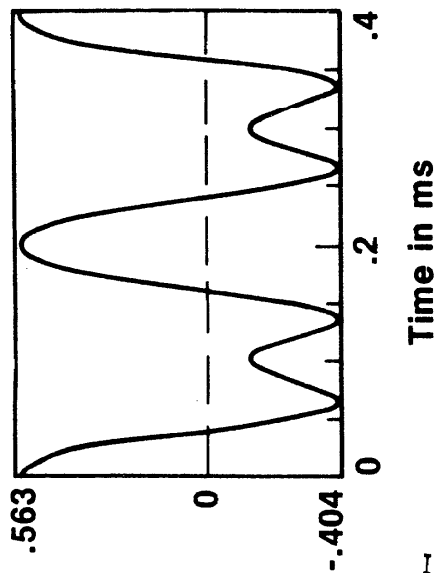
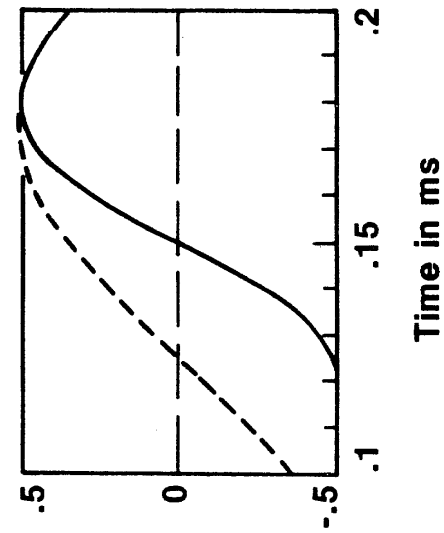
FIGURE 5. Values of $J_p(x)$, where $x=4\pi d/\lambda$, as a function of d



$$\Delta = \frac{7}{16} \lambda$$



$$\Delta = \frac{3}{8} \lambda$$



$$\Delta = \frac{5}{16} \lambda$$

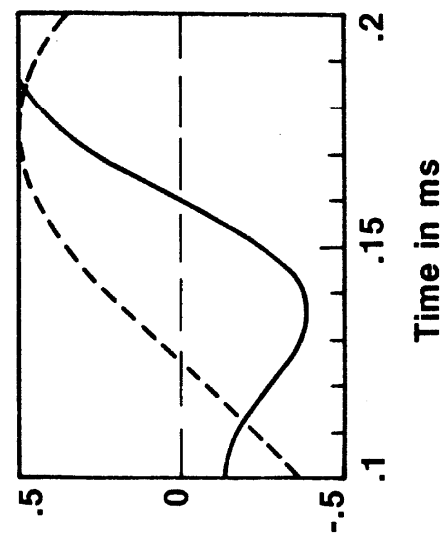


FIGURE 6. Photodetector (solid) and accelerometer (dashed) outputs at $d=92.7$ nm

the graphs in Figure 7, where the variation of phase with Δ is exhibited over the range $5\lambda/16 < \Delta < 7\lambda/16$. The number beside each line represents the average of 16 samples. Note that it agrees with the phase value for $\Delta = 3\lambda/8$. Averaging also increases accuracy by reducing the effects of random noise.

The measurement of phase, as indicated in Figure 2, immediately follows the measurement of $|S|$. The drive voltage is reduced to 0.76 of its value of fringe disappearance. This step maximizes the fundamental component and makes $d = 92.7$ nm. Next, I_{dc} is sampled to establish the point of maximum positive slope. Shortly before reaching that point, the phasemeter is commanded to take 9 readings which, if acceptable, are averaged to yield the required phase information. Since in the above discussion of phase we have used the displacement ξ , it is necessary to apply a 180-degree correction whenever the sensitivity of an accelerometer is measured. In our apparatus, this correction is built into photodetector electronics.

An alternate way to measure the phase ϕ of the sensitivity S is suggested by studying the shape of the theoretical phase-vs.-delta curve of the photodetector output. Figure 8 shows this phase behavior as Δ is changed over the range 0 to λ , for three different values of ϕ . The value of ϕ is always the phase corresponding to the mid-point of the downward sloping curve. As expected, in Figure 8 that point occurs at $\Delta = (3/8)\lambda$ and $(7/8)\lambda$. For comparison, two typical experimentally obtained curves are shown in Figure 9. Except for the spikes occurring just before the high jump in phase, they have the salient features of the curves in Figure 8. Consequently, the implementation of this approach is very direct: the phasemeter is sampled over at least two periods of the low frequency sweep. After locating the points P1 and P2 (see Figure 8), the program selects the value of the phase corresponding to the mid-point. The process is repeated several times and the results are averaged. The scatter is less than 2 degrees if the controlling parameters are properly set.

The latter approach is not only simpler, requiring only one type of measurement, but also allows a cheaper laser to be used. For the former method, a highly stable laser is essential because the phase must be read at specific times related to a specific value of the average current in the photodetector.

Regardless of the method chosen to process the phase information, the pertinent specifications of the phasemeter must be respected. The instrument used in the research reported here requires 4.6 time constants for the output to reach 99% of the true value of phase, the time constant being of the order of 10ms.

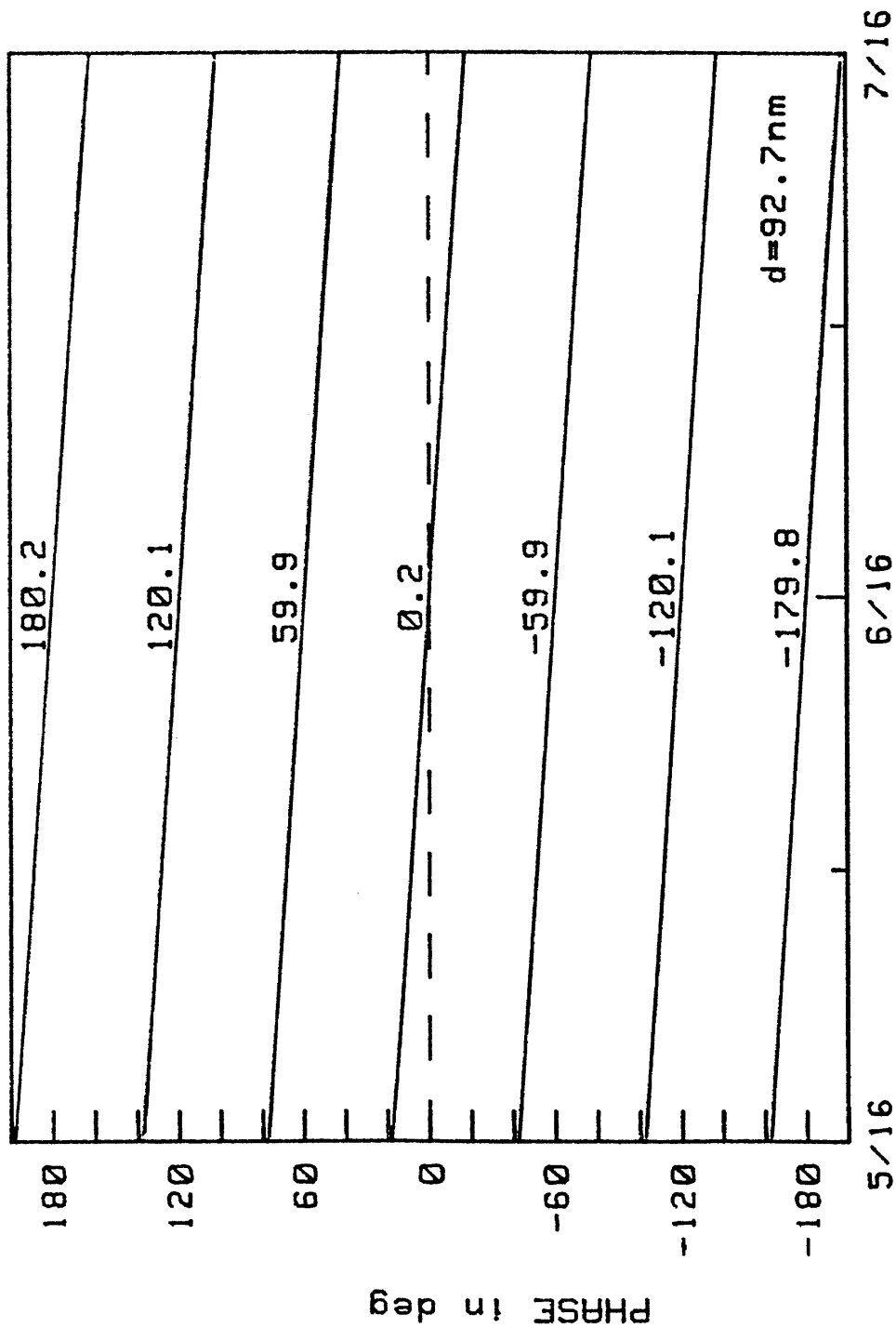
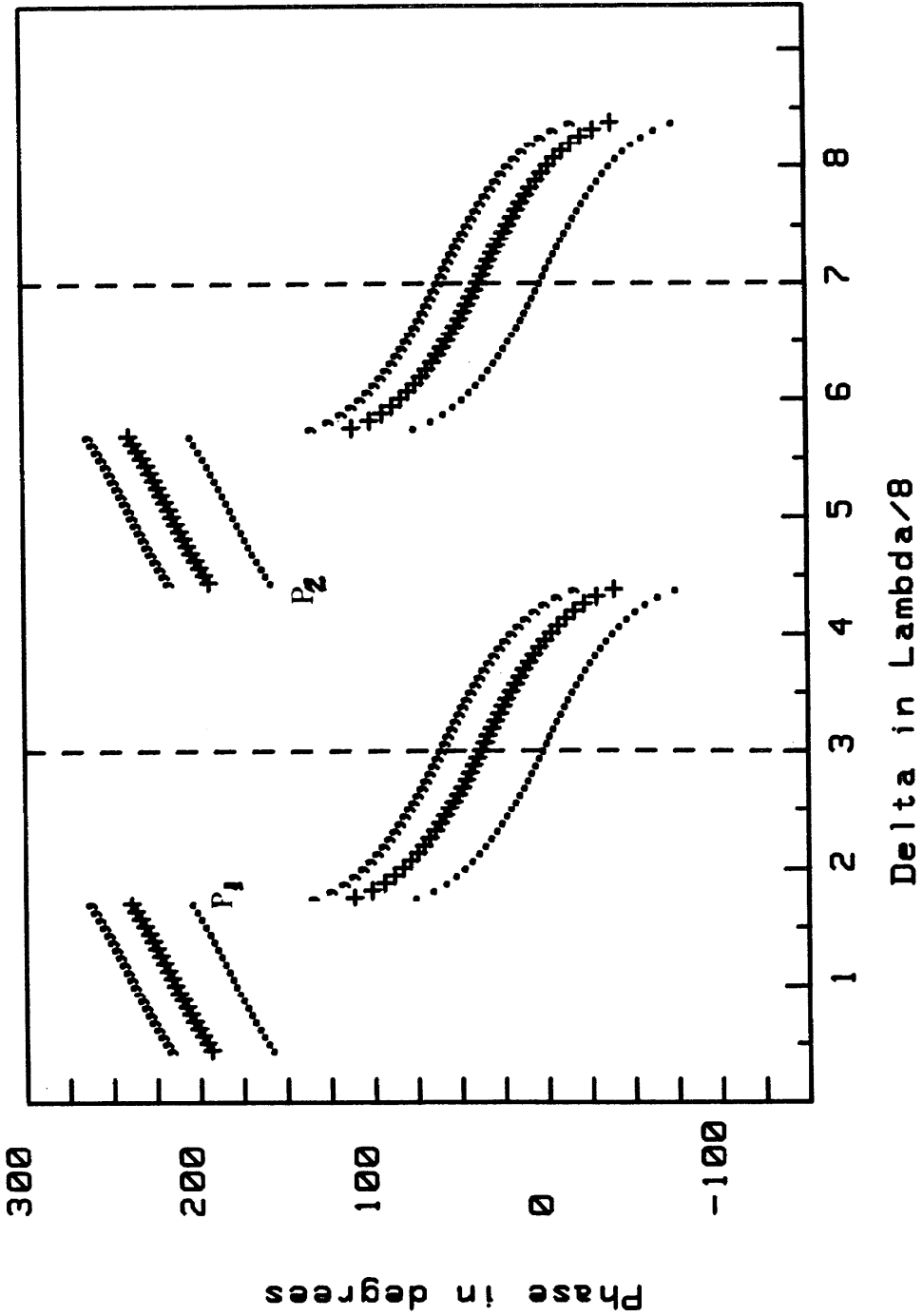


FIGURE 7. Behavior of the phase of $i r e E$ near $\Delta = \lambda/8$ for different values of ϕ

. Phi = 0 deg
 + Phi = 30 deg
 , Phi = 60 deg



**FIGURE 8. Variation of the phase of i re E with
 computed for three values of ϕ**

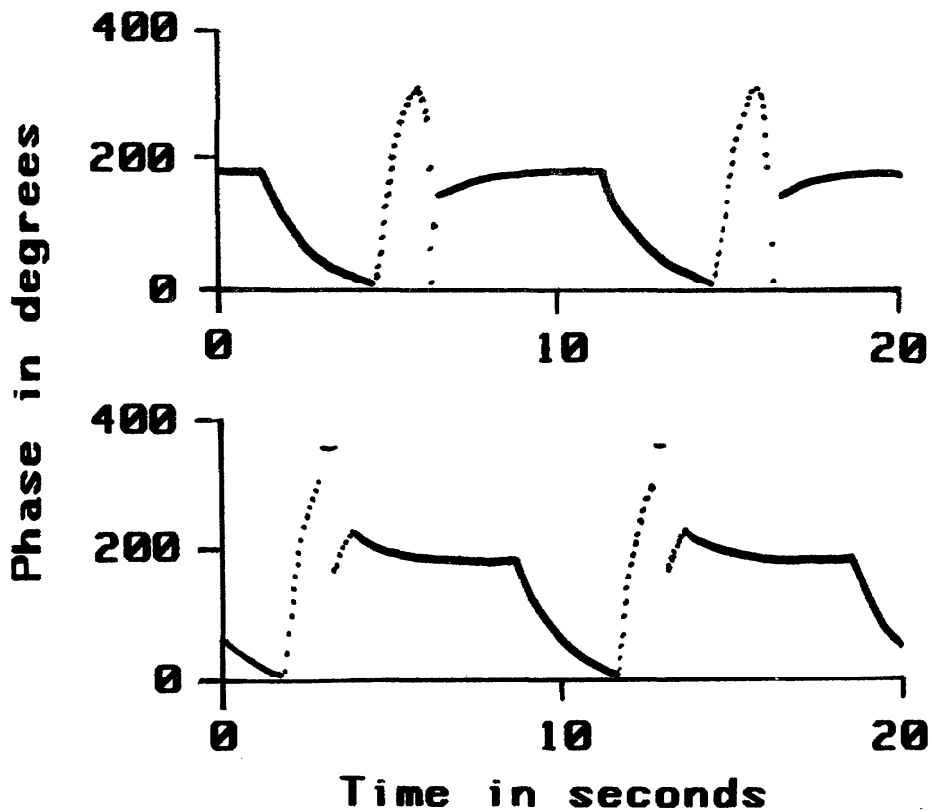


FIGURE 9. Two samples of the phase of i as Δ is varied at 0.1 Hz rate

This places a limitation on the speed with which the fixed mirror may be moved. It was, therefore, considered prudent to lower the frequency of the sweep to 0.1 Hz for the phase measurement. The only other restriction is on the amplitude of the fixed mirror motion. Again, for both of the above methods of measuring phase, the swing was limited to $\lambda/2$.

Calibration at Other Vibration Levels

The system just described was designed to measure the magnitude of S at $d=121.10$ nm. Nevertheless, it is possible to perform a calibration at higher values of d, specifically at the higher order zeros of $J_0(4\pi d/\lambda)$. Table 2 shows the results of a linearity test on a pickup, at 4000 Hz.

Table II- Linearity Check at 4000 Hz.

Order of Zero of $J_0(4\pi d/\lambda)$	Peak displacement d in nm	Magnitude of S in mV/"g"
1	121.10	10.09
2	277.97	10.13
3	435.78	10.04

The phase of S also can be measured at values of d other than 92.7 nm. Figure 4 illustrates how the phase of a linear pickup has the same value at 60 nm and 120 nm. Note that when d is appreciably larger than 121 nm, it becomes necessary to filter the photodetector output, which complicates the measurement.

PERFORMANCE TESTS

The first test consisted of ascertaining the response of the system components to changes in critical-parameter values. In particular, it was found that the smallest measurable change in displacement magnitude was less than 0.1%. This corresponds to about 0.1 nm and can be produced by a change of about 5 mV in the oscillator output, with the power amplifier gain set at less than half of its rated value. The sensitivity of the phase measurement was estimated from the slope of the curves near $\Delta=\lambda/8$ in Figure 8. It is on the order of 0.5 degree per nm. Thus, 0.1 nm variation in the optical path length difference will produce a phase change of about 0.05 degree, which is both measurable and adequate.

The noise floor for the very-low-frequency diagnostic signals sampled with the d-c voltmeter is about 1 mV. This permits a 60-dB dynamic range in $M=2BJ_0(4\pi d/\lambda)$. In terms of displacement this means that only the band 121.0 to 121.2 nm is below the noise floor.

The routine which finds the E-intercept necessary for computing the magnitude of the sensitivity was verified using

theoretical values of the Bessel function $J_0(x)$. An added measure of confidence was provided by the agreement of $|S|$ values obtained for a test accelerometer with other calibration results. Figure 10 illustrates this. The results of the comparison calibration with a NBS standard accelerometer are plotted as little squares; the crosses represent the values obtained by the method of this paper. The agreement is within 1% over the frequency range 3-8 kHz. Below 3 kHz the comparison calibration is considered more accurate, and above 8 kHz, the interferometric calibration.

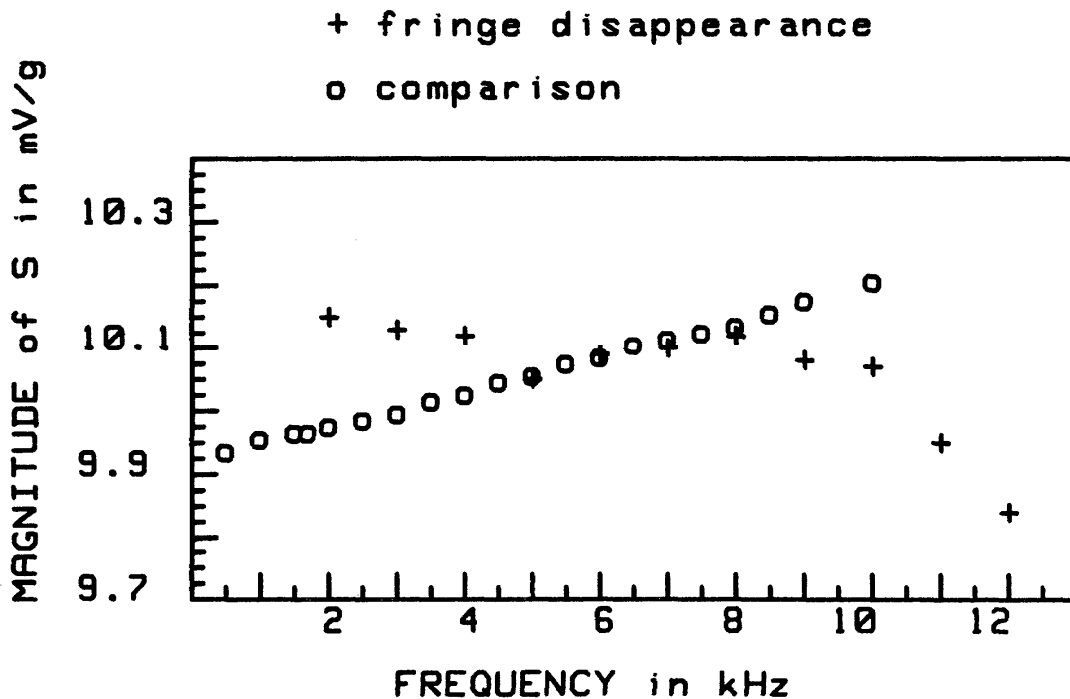


FIGURE 10. Accelerometer sensitivity $|S|$ of a test accelerometer with charge amplifier

To qualify the system as a phase measuring instrument, two tests were performed. The first test consisted of inserting a phase shifter between the oscillator and the amplifier used to drive the vibration exciter (see Figure 1), and measuring the phase of the displacement ξ relative to the oscillator output E_{dr} .

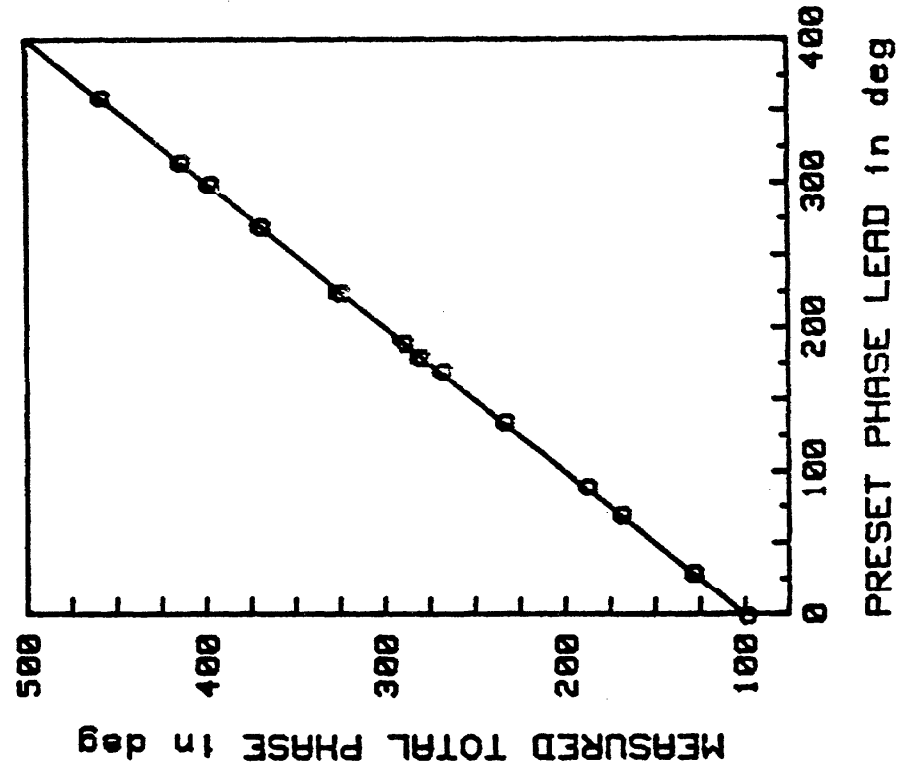


FIGURE 11. Test of the systems' accuracy in measuring phase differences

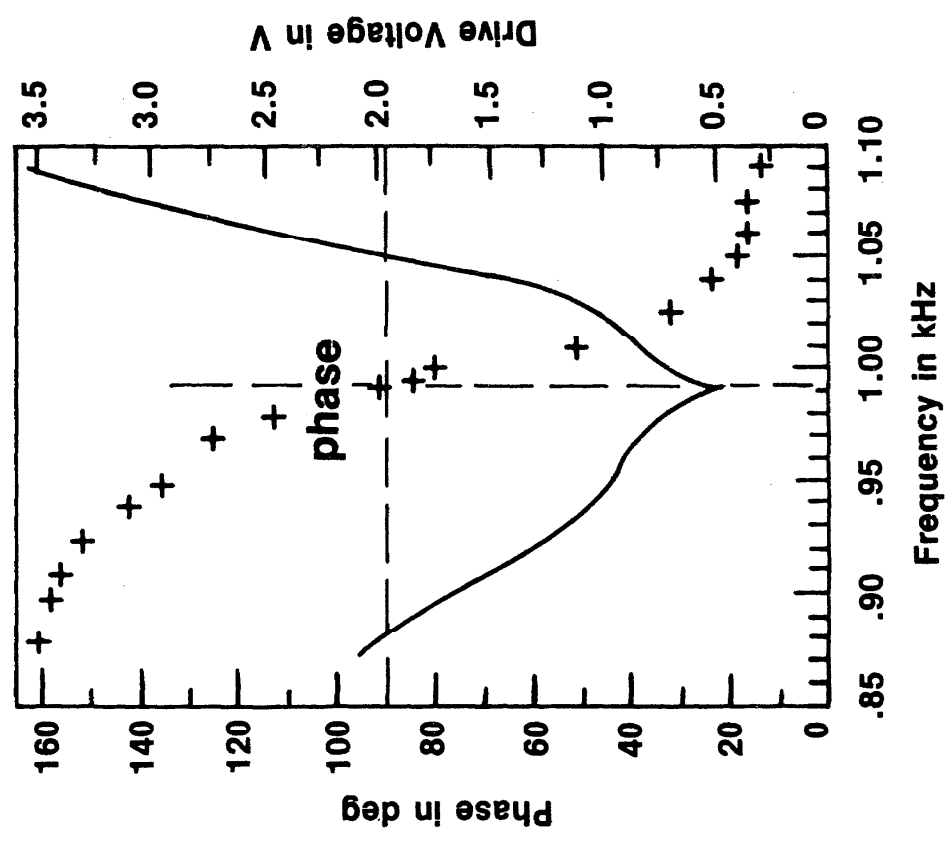


FIGURE 12. Behavior of a piezo electric transducer near its first resonance, at $d \approx 92.7$ nm

The resultant phase, plotted in Figure 11, always increased by the amount added by the phase shifter. This test proved that the system can accurately measure changes in phase between 0 and 360 degrees. The second test was to measure a phase angle precisely known from physical principles. Such a test was devised using the first resonance of a piezoelectric cylinder, when the displacement is 90 degrees out of phase with the applied voltage [13]. Figure 12 presents the results of the test, performed at a constant displacement amplitude of about 92.7 nm. The 90-degree value of phase occurs at the same frequency as the dip in the resonance curve.

Figure 13 shows the results of phase calibrations by the method of this paper (crosses) and by comparison with a NBS standard accelerometer (squares). The test transducer is the one used for the magnitude-of-S calibrations presented in Figure 10.

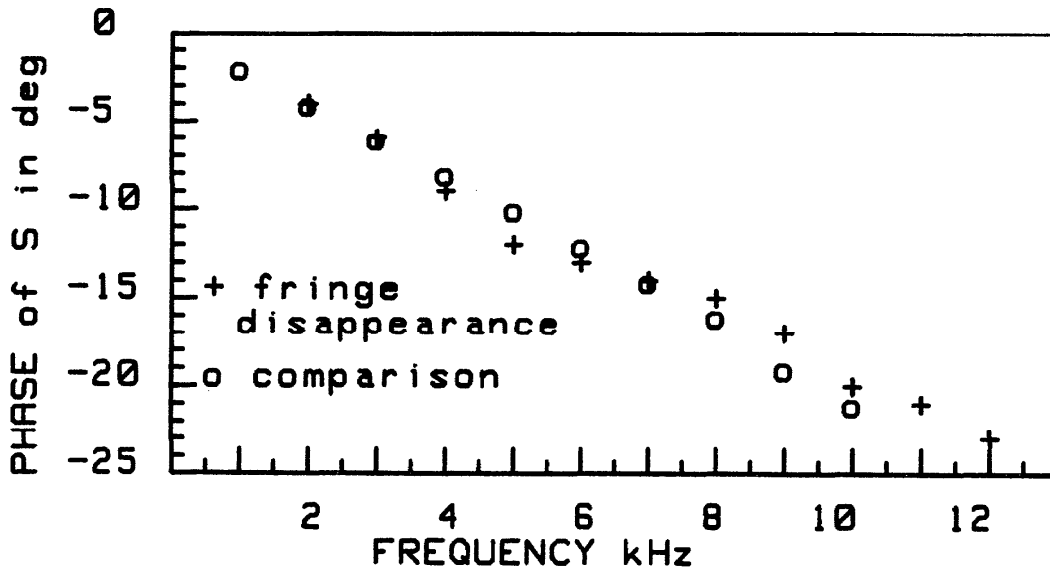


FIGURE 13. Phase calibration of a test accelerometer with charge amplifier

CONCLUDING REMARKS

The classical fringe-disappearance technique of optical interferometry has been developed into an automated procedure for absolute calibration of vibration pickups.

The new method uses only the d-c component of the photodetector output in a Michelson interferometer to set the vibration exciter precisely at 121.10 nm peak displacement. By also measuring the electrical output of the pickup, the magnitude of its sensitivity is calculated.

The phase component of the pickup sensitivity is extracted from the measurement of the phase of the pickup signal with respect to the unfiltered photodetector output. This part of the calibration is most conveniently done at a displacement amplitude of about 90 nm.

The dynamic measurement of phase, achieved by a controlled continuous variation of the optical path length, besides being convenient for automation, makes the method more generally applicable. It removes the need to know the static length difference of the optical paths. The determination and stabilization of that quantity can be very difficult or impracticable[14,15].

The frequency range is determined primarily by the characteristics of the vibration exciter. Most of our measurements so far have been in the range 1 to 10 kHz.

Although the results have been highly repeatable, at the present time only a 2% accuracy is claimed for the magnitude and ± 2 degrees for the phase measurement because of the limited amount of data collected to date.

ACKNOWLEDGEMENT

Mai-Huong Nguyen provided programming and computation assistance; her help in the preparation of the final copy is also gratefully acknowledged.

REFERENCES

1. A. G. Webster, Proc. Nat. Acad. Sci. (USA) 5, 173(1919).
2. H. A. Thomas and G. W. Warren, Phil. Mag., Series 7, 5, No. 32 (1928).
3. H. Osterberg, Proc. Nat. Acad. Sci. (USA) 15, 892(1929).
4. H. Osterberg, J. Opt. Soc. Amer., 22, 19(1932).
5. W. J. Kennedy, J. Opt. Soc. Amer., 31, 99(1941).
6. D. A. Smith, Proc. Phys. Soc. (London), 57, 534(1945).
7. V. A. Schmidt, et al., J. Acoust. Soc. Am., 34, 455(1962).
8. M. R. Serbyn, Doctoral Dissertation, Catholic Univ. of America(1971).
9. M. R. Serbyn and B. F. Payne, J. Acoust. Soc. Am., 68, Suppl. 1, S75(1980).
10. M. R. Serbyn, Proc. 1st Internat. Modal Analysis Conf., (spons. by Union College), 223-229(Nov. 8-10, 1982).
11. IEEE Standard Dictionary of Electrical and Electronics Terms, p. 1, IEEE, Inc., (1977).
12. M. R. Serbyn and F. A. Andrews, J. Acoust. Soc. Am., 46, 2-5(1969).
13. L. L. Beranek, Acoustics, p. 86, McGraw-Hill(1954).
14. G. Lauer, Fortschritte der Akustik DAGA'81, VDE Verlag(1981).
15. G. Lauer, Fortschritte der Akustik DAGA'80, 811-814, VDE Verlag(1980).